

ANALYSIS OF INFLUENCE OF SPEED VARIATION OF HIGH SPEED BALL BEARINGS ON CAGE DYNAMIC PERFORMANCE

高速球轴承转速变化对保持架动态性能影响分析

Ass. Prof. Ph.D. Eng. Ye Zhenhuan^{1,2)}, Prof. Ph.D. Eng. Wang Liqin^{*2)}, Ph.D. Eng. Zhang Chuanwei^{2,3)}

¹⁾ School of Engineering, Zunyi Normal College, Zunyi / China; ²⁾ School of Mechatronics Engineering, Harbin Institute of Technology, Harbin / China; ³⁾ Nano-Tribology of Discrete Track Recording Media, University of California, San Diego, La Jolla / United States

Tel: +8645186402012; Email: lqwanghit@gmail.com

Abstract: With the aim of increasing the stability of high-speed ball bearings in the transmission system of agricultural machinery, taking a type 7004 high speed angular contact ball bearings as the research material, a dynamic model of high speed ball bearings was built based on the geometry and force relationship of bearing elements. The integration method used by Runge-Kutta and Newton-Raphson is proposed to efficiently solve the nonlinear equations. The accuracy of the dynamic model constructed in this paper was verified by the testing and computation results studied by Gupta. A computation program is developed and the cage stability at different bearing rotation speeds is studied. The results shown that the increase of bearing rotation speed has improved both the cage stability and cage sliding ratio. In addition, the impact between the cage pocket and the ball has a serious effect on cage stability when the bearing is in the starting process. This study provides support for the design of working conditions and failure analysis of ball bearings, as well as a theoretical basis for analysis of the system stability of transmission systems in agricultural machinery.

Keywords: High speed ball bearings; Dynamic; Cage stability; Static condition; Transitional condition

INTRODUCTION

With developments in modern agricultural machinery moving toward lightweight and intelligent designs, the reliability and stability of agricultural machinery transmission systems has gradually become an area of focus [13,14,16]. Over the years, many researchers have studied the rolling bearings in the transmission systems of agricultural machinery in terms of two aspects: a detection technique for bearing faults [4,11,22] and predictions and simulations which focus on the influence of bearing structure on performance [1,2,5,21]. However, those simulation analyses only consider the loading properties of the bearing and rarely involve the dynamic stability of the bearings.

The dynamic performance of high-speed rolling bearings in these transmission systems not only affect their own life and stability, but also relates to the vibration and reliability of the rotor system. In order to understand the dynamic performance of the bearings during operation, a fully dynamic analysis of the bearings is needed. Over the years, much research has been done on the dynamic characteristics of high-speed ball bearings. In particular, with regard to the force and motion analysis of cage, Gupta developed the influence of cage clearance on bearing stability [7], while Weinzapfel et al. [17] also analyzed and compared the effects of rigid and flexible cage on bearing stability. In addition, Bai [3] and Liu [19] also studied the dynamic characteristics of the bearings in terms of the waviness and cage clearance ratio of angular contact bearings.

However, previous studies on high-speed rolling

摘要: 针对农机传动系统中高速球轴承的稳定性问题, 根据高速球轴承内部的几何位置关系以及相互作用力关系, 以 7004 型高速角接触球轴承作为研究对象, 建立了高速球轴承的动力学模型。采用 Runge-Kutta 法和 Newton-Raphson 法混合求解的思想对模型非线性方程组进行了高效求解。采用 Gupta 的实验和仿真结果验证了本文模型和方法的可靠性。从轴承稳态和瞬态过渡两种工况角度研究了轴承转速变化对保持架动态性能的影响规律, 结果表明轴承转速增加有利于保持架的稳定但同时增大了保持架滑动率; 变速过程中, 保持架在启动阶段产生的兜孔和滚动物体频繁冲击对其稳定性影响较大。研究结果为高速球轴承在设计计算以及失效分析等方面提供有力的支持, 并为传动系统的系统稳定性分析提供了理论基础。

关键词: 高速球轴承; 动力学; 保持架振动; 稳态工况; 瞬态过渡工况

引言

随着现代农业机械朝着轻量化和智能化方向的发展, 农机传动系统的可靠性和稳定性逐渐成为农机设计和使用的重点关注内容[13,14,16]。多年来, 许多学者对农机传动系统中的滚动轴承进行了研究, 一方面是集中在针对轴承故障进行检测技术的研究[4,11,22], 另一方面集中在轴承结构对性能影响的仿真预测分析[1,2,5,21], 但是仿真分析多考虑到轴承承载性能而很少涉及到轴承动态稳定性。

农机传动系统中高速滚动轴承的动态性能不仅影响其自身的寿命和稳定性, 还关系到转子系统的振动和可靠性。为了清楚的研究轴承在工作过程中的动态性能必须对轴承进行完全动力学分析。多年来, 国内外的众多学者在高速球轴承的动力学方面做了大量的研究工作, 特别是针对保持架受力运动分析 Gupta 专门讨论了保持架间隙对轴承稳定性的影响[7], Nick Weinzapfel 等[17]还分析对比了保持架刚性和柔性对轴承稳定性的影响。国内的白长青[3]、刘秀海[19]等也针对角接触球轴承的波纹度、保持架间隙比等情况研究了轴承的动态特性。但是通过分析可以发现, 对于农机传动系统高速滚动轴承的研究基本都局限

bearings in these transmission systems are limited to the basic dynamic performance analysis of different steady state conditions and have rarely ever investigated the dynamic properties of the bearing in the variable transition process. Frequent impact of the cage and the rolling elements during transmission operation directly affects the dynamic stability of the cage and ultimately influences the stability and reliability of transmission systems in agricultural machinery.

In this paper, through the establishment of a dynamic analysis model and development of an efficient dynamics program, the effect of velocity changes of high-speed ball bearings on the dynamic performance of the cage was analyzed and discussed. The results support the improvement of the design computation and failure analysis of high-speed rolling bearings in agricultural machinery transmission systems.

MATERIAL AND METHOD

Research materials

7004 angular contact ball bearings are used in this paper as the research material, their material and geometry parameters being shown in Table 1 and Table 2. The lubrication oil type MIL-L-7808 is used. The axial load F_x and radial load F_z on the bearings are 2000 N and 400 N, respectively.

于不同稳态工况下的动态性能分析，对于农机传动系统在变工况过渡过程中高速轴承的动态性能研究较少，而轴承在工况变化过程中保持架和滚动体的频繁冲击直接影响着保持架的动态稳定性，进而影响到整个农机传动系统的稳定性和可靠性。

本文通过建立球轴承的动力学分析模型，开发高效的动力学程序，对高速球轴承转速变化对保持架动态性能的影响进行分析和讨论，为农机传动系统高速球轴承在设计计算以及失效分析等方面提供有力的支持。

材料与方法

研究材料

本文将 7004 型角接触球轴承作为研究材料进行分析，具体的结构参数和材料参数如表 1 和表 2 所示，润滑采用 MIL-L-7808 型润滑油。轴承承受轴向载荷和径向载荷分别为 2000N 和 400N。

Table 1

Material parameters of ball bearings [7]

Elements	Density [kg/m ³]	Elastic modulus [GPa]	Poisson's ratio [-]
Ball	3200	310	0.260
Rings	7750	200	0.250
Cage	1500	1.73	0.300

Table 2

Geometry parameters of ball bearings [7]

Geometry parameter	u.m.	Value
Pitch diameter	[mm]	31
Ball diameter	[mm]	8
No. of balls	[-]	6
Contact angle	[°]	24
Inner curvature factor	[-]	0.56
Outer curvature factor	[-]	0.52
Cage inner diameter	[mm]	30
Cage outer diameter	[mm]	35
Cage pocket clearance	[mm]	0.1
Cage guiding clearance	[mm]	0.25

Analysis Method

The contact load Q between the raceways and the balls are calculated by the Hertz contact theory [10], so the contact load between the j^{th} rolling element and the raceways is expressed as:

$$Q_j = K_j \delta_j^{3/2} \tag{1}$$

where the stiffness K is calculated according to the study by Johnson [10], and the contact deformation δ is determined by the positional relationship between the rolling element and the raceway as shown in Fig. 1. Thus, the contact deformation δ_j between the j^{th} rolling element and the raceway is expressed by the vector $\mathbf{O}_{rj}\mathbf{O}_{bj}$ which means that the center of the raceway to the center of the ball, the groove curvature coefficient f of the ring, and the diameter of the ball D_w are expressed as:

分析方法

套圈滚道和滚动体之间的接触载荷 Q 采用赫兹接触理论计算[10]，第 j 个滚动体和滚道之间的接触载荷表示为：

式中的刚度 K 根据文献[10]计算，接触变形 δ 根据如图 1 所示的滚动体和套圈滚道之间的位置关系确定，其中第 j 个滚动体和套圈滚道之间的接触变形 δ_j 由套圈滚道中心到球中心的矢量 $\mathbf{O}_{rj}\mathbf{O}_{bj}$ 、套圈的沟曲率系数 f 表示和滚动体直径 D_w 表示为：

$$\delta_j = (f - 0.5) \cdot D_w - |\mathbf{O}_{rj} \mathbf{O}_{bj}| \tag{2}$$

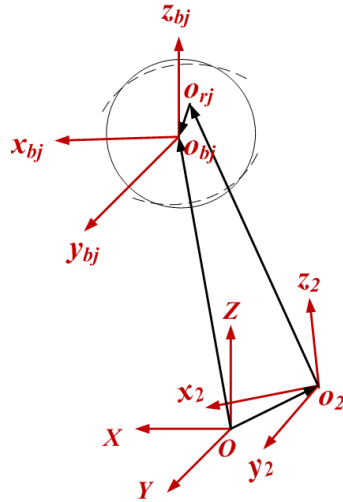


Fig. 1 - The sketch of the displacement of raceway and ball

The traction force F_μ of the contact area is equal to the traction coefficient μ multiplied by the contact load Q . The traction coefficient formula [20] is:

接触区的拖动力 F_μ 等于拖动系数 μ 和接触载荷 Q 的乘积，拖动系数公式为[20]:

$$\mu = (A + Bs)e^{-Cs} + D \tag{3}$$

where s is the slip-roll ratio which could be obtained from the kinematic analysis. Coefficients A , B , C , and D are calculated according to the formula in the study by Wang [20].

式中 s 为滑滚比，由运动学分析计算得到，系数 A 、 B 、 C 、 D 按文献[20]中公式计算。

Fig. 2 shows the relative position relationship between the rolling element and the cage pocket. According to the vector $\mathbf{O}_{pj} \mathbf{O}_{bj}$ between the cage pocket and the center of the ball bearing and the initial clearance between the cage pocket and the ball bearing Δ_{bp} , the minimum clearance δ_{bp} can be expressed as follows:

图 2 所示为滚动体和保持架兜孔之间的相对位置关系，根据保持架兜孔中心到球心的向量 $\mathbf{O}_{pj} \mathbf{O}_{bj}$ 和保持架兜孔和滚动体之间的初始间隙 Δ_{bp} ，最小间隙 δ_{bp} 可以表示为:

$$\delta_{bp} = \Delta_{bp} - |\mathbf{O}_{pj} \mathbf{O}_{bj}| \tag{4}$$

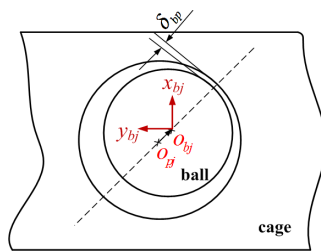


Fig. 2- The sketch of the displacement of the cage pocket and the ball bearing

According to the amplitude of the clearance between the cage pocket and the ball bearing δ_{bp} , taking into consideration both the roughness of the ball bearing ϵ_b and the cage ϵ_p , two interaction models are used:

根据球和保持架兜孔间的间隙 δ_{bp} ，考虑球的粗糙度 ϵ_b 和保持架兜孔的粗糙度 ϵ_p ，将滚动体和保持架兜孔的位置关系归纳为以下两个模型:

$$d_{bp} \in \sqrt{e_b^2 + e_p^2} \tag{5a}$$

$$d_{bp} > \sqrt{e_b^2 + e_p^2} \tag{5b}$$

If the inequality (5a) is true, the interaction is assumed to be Hertz contact. The normal load between the cage pocket and ball bearing is calculated by Hertz point contact theory [10], and the tangential load between cage pocket and the ball bearing equals the normal load multiplied by the friction coefficient.

Otherwise, if the inequality (5b) is true, the interaction is assumed to be hydrodynamic lubrication. Reynolds equations [9] are used to calculate the interaction force. The interactions in two directions, shown as Fig. 3, are assumed to be independent of each other.

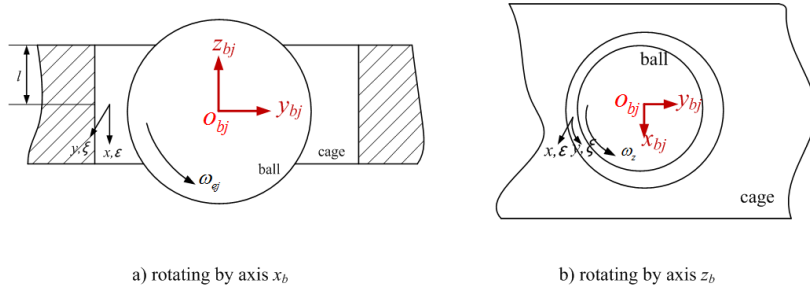


Fig. 3- Hydrodynamic effect between ball bearing and cage pocket

Fig. 4 shows the interaction between the cage and the guiding ring, and the force between the two can be approximated as the fluid dynamic pressure of the journal bearing. As the contact surface of the ring flange and cylinder surface of the cage is relatively small, the short journal bearings model [18] is adopted.

若滚动体和保持架兜孔满足 (5.a) 模型, 二者之间的相互作用为赫兹接触。根据赫兹点接触理论[10]计算二者间的法向力, 二者间的切向力等于法向力乘以摩擦系数。

若滚动体和保持架兜孔满足 (5.b) 模型, 二者之间的相互作用为流体动压。根据雷诺方程[9]计算二者间的作用力, 其中如图 3 所示的两个方向的流体动压作用假设为不相关函数。

图 4 所示为保持架和引导套圈之间的作用, 套圈挡边引导面与保持架引导面间的作用力可以近似为滑动轴承计算中的流体动压力, 由于挡边与保持架柱面间的作用面比较小, 故通常采用短滑动轴承模型[18]。

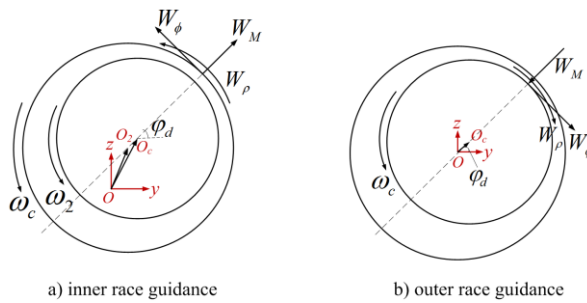


Fig. 4- The interaction between cage and guiding ring

$$\begin{aligned}
 W_M &= \pm \frac{\eta R_g B_g^3}{C_g^2} \frac{\varepsilon^2}{(1-\varepsilon^2)^2} (\omega_{1,2} + \omega_c) \\
 W_\phi &= \pm \frac{\pi \eta R_g B_g^3}{4 C_g^2} \frac{\varepsilon}{(1-\varepsilon^2)^{3/2}} (\omega_{1,2} + \omega_c) \\
 W_\rho &= \frac{2 \pi \eta R_g^3 B_g}{C_g} \frac{1}{\sqrt{1-\varepsilon^2}} (\omega_{1,2} - \omega_c)
 \end{aligned} \tag{6}$$

Where:

W_M , W_ϕ , and W_ρ are the normal force, tangential force, and moment between the cage and the guiding ring. η is the viscosity of the oil. R_g and B_g are the radius and the width of the guiding surface. C_g is initial clearance of the bearings. ε is the eccentricity ratio of the cage center. ω is that rotational speed of the element. Subscripts 1, 2, and c represent the outer ring, inner ring, and cage, respectively. The sign of the equations is negative while the cage with outer race guidance.

According to the interaction angle between the cage and the ring ϕ_d , the interaction force could be expressed as equation (7) through a coordination transformation.

式中, W_M , W_ϕ 和 W_ρ 分别代表保持架和套圈引导面之间的法向力、切向力以及转矩。 η 为润滑油粘度。 R_g 和 B_g 代表引导面直径及宽度。 C_g 为轴承初始游隙。 ε 为保持架的偏心率。 ω 是轴承元件的转速。下标 1、2 和 c 分别代表外圈、内圈和保持架。若保持架由外圈引导, 计算式前取负号, 否则取正号。

根据保持架和套圈引导面之间的作用角 ϕ_d , 通过坐标变换将二者之间的作用力变换为固定坐标系下的表达式, 如式 (7) 所示。

$$\begin{bmatrix} F_y \\ F_z \\ M_l \end{bmatrix} = \begin{bmatrix} \cos \varphi_d & -\sin \varphi_d & 0 \\ \sin \varphi_d & \cos \varphi_d & 0 \\ 0 & 0 & 1 \end{bmatrix} \begin{bmatrix} W_M \\ W_\phi \\ W_\rho \end{bmatrix} \quad (7)$$

Solution method

In addition to the interaction force, the bearing lubricant retarding force F_D and retarding moments M_e , which can be calculated by Schlichting's fluid theory [15], should also be taken into consideration. Forces of the loaded rolling element are shown in Figure 5. In the figures, M_{μ} and M_{bp} are the traction moment between the raceway and the rolling element and friction moment between the cage and the rolling element, respectively. The motion equation of the j^{th} rolling element centroid and of its revolving around the centroid is determined by its resultant force and the moment as shown in equation (8).

求解方法

轴承套圈、保持架以及滚动体除了相互作用力，还需要考虑轴承中润滑油的阻滞力 F_D 和阻滞力矩 M_e ，根据 Schlichting 的流体理论进行计算[15]。考虑所有载荷的滚动体受力情况如图 5 所示，其中 M_{μ} 和 M_{bp} 分别为滚道/滚动体之间拖动力矩及保持架/滚动体之间摩擦力矩。第 j 个滚动体质心的运动方程和绕质心的运动方程分别根据第 j 个滚动体所受的合力和合力矩确定，如式 (8) 所示：

$$\begin{aligned} F_{\mu j} - F_{Dj} + F_{bpjy} &= m_b r_b \ddot{\theta}_j \\ M_{bpjx} - M_{ejx} + M_{\mu jx} &= I_b \dot{\omega}_{yj} \\ M_{bpjy} - M_{ejy} + M_{\mu jy} &= I_b \dot{\omega}_{xj} \\ M_{bpjz} - M_{ejz} + M_{\mu jz} &= I_b \dot{\omega}_{zj} \end{aligned} \quad (8)$$

where, m_b and I_b are the mass and rotary inertia of ball. r_b is the revolution radius of ball. θ is the azimuth angle of ball and ω is the rotation speed of ball. Subscript j represents the parameter j^{th} ball. Subscripts x, y, and z represent the components in each of the three directions.

式中 m_b , I_b 分别表示球的质量和转动惯量， r_b 表示球的公转半径， θ 表示球的方位角， ω 表示球的转速。下标 j 表示第 j 个滚动体；下标 x、y、z 表示 x、y、z 三个坐标方向的分量。

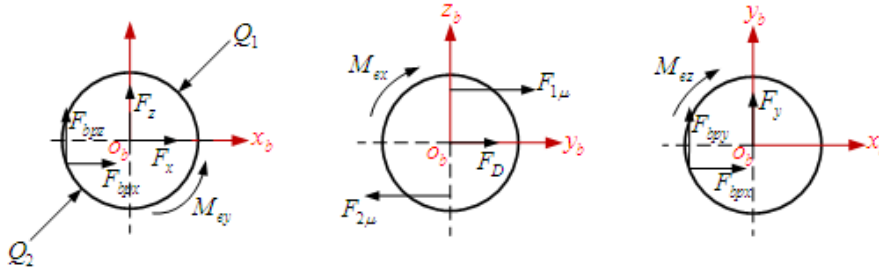


Fig. 5 - Forces and moments acting on ball.

To eliminate high-frequency vibrations generated by contact between a ball bearing and rings, a balance constraint is adopted for the contact between the ball and the ring. First, nonlinear equilibrium equations with the quasi-dynamic method are established, and the Newton-Raphson method is used to solve the equations [12].

为消除球和套圈接触产生的高频振动，球和套圈之间接触采用平衡约束，通过拟动力学的分析方法建立非线性平衡方程组并采用 Newton—Raphson 方法求解 [12]。

Similarly, based on the force condition, the differential equations of the cage can be listed as equation (9). Where, n is the ball number. m_c and I_c are mass and rotary inertia of cage. x_c , y_c and z_c are displacement of cage mass center on direction x, y and z. θ_c is the relative rotation angle between cage mass center and bearing center.

同理，对于保持架可以根据其受力情况列出其运动微分方程如式 (9) 所示，其中 n 表示球数， m_c 和 I_c 表示保持架质量和转动惯量， x_c 、 y_c 和 z_c 表示保持架质心在 x、y 和 z 方向的位移， θ_c 表示保持架质心相对轴承中心的转角。

$$\begin{aligned} \sum_{j=1}^n (-F_{bpjx}) &= m_c \ddot{x}_c \\ F_{ly} + \sum_{j=1}^n (-F_{bpjy} \cdot \cos \theta_j - F_{bpjz} \cdot \sin \theta_j) &= m_c \ddot{y}_c \\ F_{lz} + \sum_{j=1}^n (-F_{bpjy} \cdot \sin \theta_j - F_{bpjz} \cdot \cos \theta_j) &= m_c \ddot{z}_c \\ \sum_{j=1}^n \left(-F_{bpjy} \cdot \frac{D_c}{2} \right) + M_l &= I_c \ddot{\theta}_c \end{aligned} \quad (9)$$

Based on simultaneous motion differential equations of the ball bearing and cage, one should use non-dimensional quantities to the parameters of the equation in formula (10), and resolve the non-dimensional differential equations with the adaptive step size fourth-order Runge-Kutta method. A stationary solution is obtained by the quasi-dynamic method as the initial values of whole solution process. The calculation procedure is shown in Fig. 6.

$$\bar{F} = \frac{F}{F_x} \quad \bar{m} = \frac{m}{m_b} \quad \bar{r} = \frac{r}{D_w/2} \quad \bar{t} = \frac{t}{\sqrt{m_b \cdot D_w / (2F_x)}} \quad (10)$$

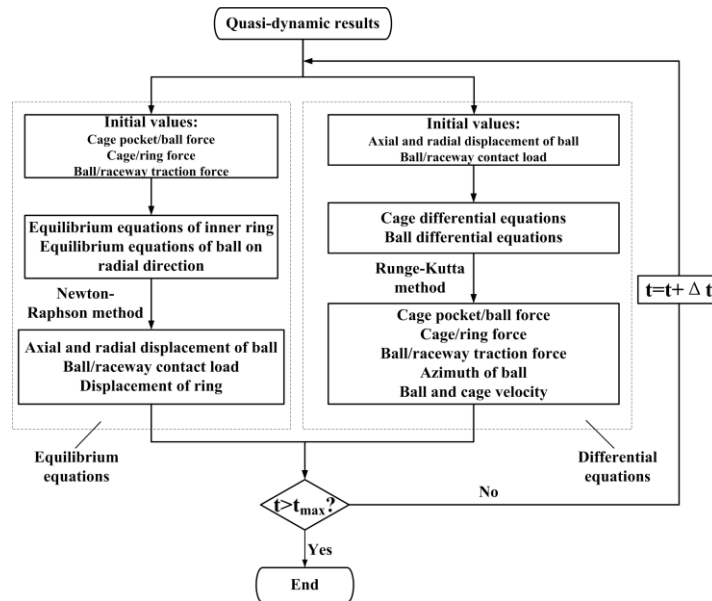


Fig. 6 - Calculation flow chart of dynamic equations

Model validation method

Taking a certain type of angular contact ball bearings as used in Gupta's experiment, the reliability verification on the bearing dynamic model is carried out. The axial load of the bearing is 4448 N, the working velocity is 20000rot/min, and other specific parameters are those used in the reference [8].

Fig. 7 shows the results of the cage mass center orbit simulated by Gupta's experimental and theoretical work. Fig. 8 shows the results of the cage mass center orbit and the ratio of the cage epicycle speed and bearing speed simulated in this study.

模型验证方法

以 Gupta 实验的某型角接触球轴承为算例，对建立的轴承动力学模型进行可靠性验证。轴承承受轴向负荷 4448N，工作转速 20000r/min，其他具体参数见文献[8]。

图 7 所示为 Gupta 实验和仿真获得的保持架涡动轨迹，图 8 所示为本文模型仿真获得的保持架涡动轨迹以及保持架质心涡动速比。

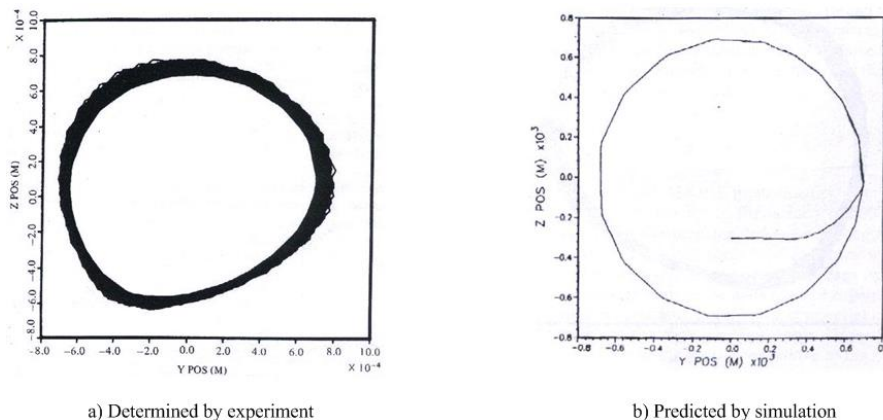


Fig. 7- Cage mass center orbit determined by Gupta [8]

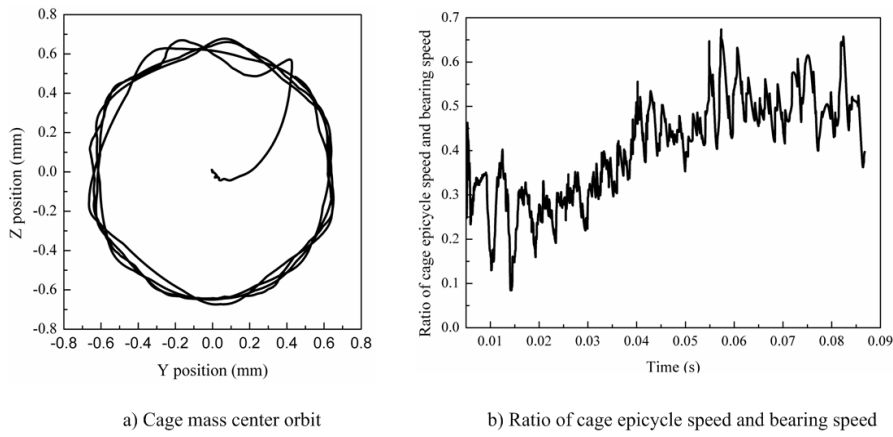


Fig. 8 - Cage mass center orbit and cage speed ratio predicted in this study

It can be seen that there is good agreement between the shape of the experimental orbit and the theoretical prediction. In addition, according to the ratio of cage epicycle speed and bearing speed simulated in this study, the range of the cage speed ratio is 0.4-0.65 when the cage whirl tends to be stable. Also, the range of the cage speed ratio determined by Gupta's experiment and theory is 0.37-0.50 and 0.31-0.35, respectively [10]. It can be seen that errors exist between the experimental work and theoretical work on the ratio of the cage epicycle speed and bearing speed, but the errors are in the acceptable range.

RESULTS AND DISCUSSIONS

Effect of bearing velocity on the dynamic performance of the cage

Fig. 9 shows the cage whirl track when the velocity of the bearing is 30000 r/min, 60000 rot /min, 80000 r/min, and 120000 r/min. In the figure, axes indicate dimensionless displacement, which is defined as the ratio of actual displacement of the cage mass to the guiding clearance of the cage. As shown in the figure, with the increase in the revolving velocity of the inner ring, the whirl track of the cage becomes regular.

从涡动轨迹上看, 本文模型仿真结果与 Gupta 实验及仿真获得的结果较为一致。从本文仿真得到的保持架质心涡动速度比可以看出, 保持架涡动趋于稳定时的速度比变化范围在 0.4~0.65 之间, 而 Gupta 通过实验以及仿真获得的保持架质心涡动速度比变化范围分别为 0.37~0.50 以及 0.31~0.35[10]。比较可知, 仿真结果和实验结果之间存在误差, 但是在可接受的范围内。

结果分析与讨论

不同轴承转速对保持架动态性能影响

图 9 所示为轴承在 30000r/min、60000r/min、80000r/min、120000r/min 四种不同转速下保持架的质心涡动轨迹, 坐标轴表示无量纲位移, 定义为保持架质心实际位移值除以保持架引导间隙值。从图中可以看出, 随着内圈转速的增大, 保持架质心的涡动轨迹逐渐规则。

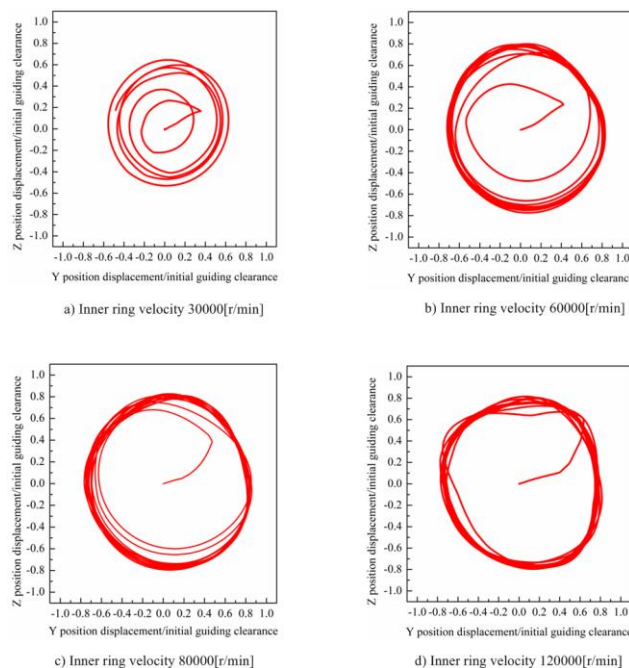


Fig. 9 - Cage whirl motion at different bearing operation speeds

According to the criteria of Ghaisas et al. [6], cage instability can be determined by the calculation of the deviation ratio σ of the whirl velocity which is defined as the ratio between the standard deviation value and average value of the velocity vector as shown in eq. (11).

$$\sigma = \frac{\sqrt{\sum_{i=1}^N (v_i - v_m)^2 / N}}{v_m} \tag{11}$$

Where, N is the number of sampling. v_m is the average speed of cage mass center.

Figure 10 shows the deviation ratio of cage whirl velocity at four different velocities. A comparison shows that with the increase of the rotational velocity of the bearings, the deviation ratio of cage whirl velocity reduces, indicating the gradual stability of the cage. The main reason for this stability is that the increase in velocity causes the cage to be pushed against the guide surface of the ring quickly under the force of the rolling element, during which the cage reaches a new balance. Meanwhile, the increase in velocity also helps to enhance the centrifugal force, which gradually increases the guiding force of the ring to the cage. Therefore, the cage whirl track tends to be stabilized.

根据 Ghaisas 等人的判断标准[6]，保持架质心涡动的不稳定性可以通过计算保持架的涡动速度偏差比 σ 来进行量化判定，速度偏差比定义为速度向量的标准偏差值与其平均值之比：

式中， N 表示采样的点数， v_m 表示保持架质心运动的平均速度。

图 10 所示为四种不同转速下的保持架涡动速度偏差比，比较可知，随着轴承转速的提高，保持架的涡动速度偏差比逐渐减小，说明保持架的稳定性逐渐增强。其主要原因为转速的上升促使保持架在滚动体的作用下被迅速推向套圈引导面获得新的平衡，另外随着转速增加带来的离心力升高促使套圈引导面对保持架的引导作用也逐渐增强，这两方面同时促使保持架质心涡动趋于稳定。

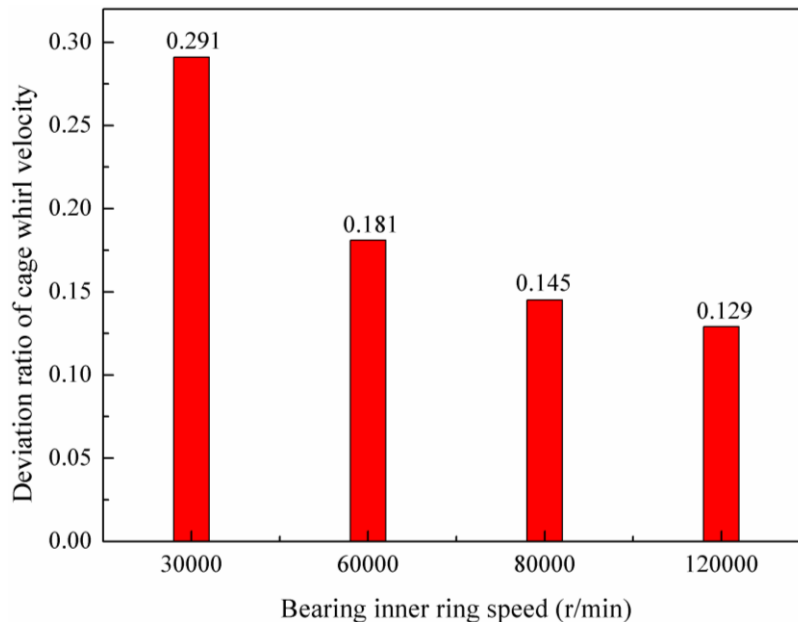


Fig. 10 - Stability of cage at different bearing operation speeds

The vibration spectrum of cage mass center at four different bearing velocities is shown in Figure 11. A comparison of the vibration frequency and the characteristic frequency of the cage mass center shows that whirl frequency of the cage mass center is always near to its revolving frequency. Also, with the increase in the bearing velocity, the whirl frequency of the cage mass center is higher than its revolving frequency at first and then gradually decreases. Therefore, to avoid having the contact between the cage and the guiding ring restricted in only one place or several places which would cause rapid wear of the cage, the relationship between the vibration frequency of cage mass center and the main frequency, the sub-frequency, and the multi-frequency of the cage revolution must be known.

在四种不同轴承转速下的保持架质心振动频谱如图 11 所示。将保持架质心振动频率和保持架特征频率进行对比可知，保持架质心涡动频率始终处于保持架转动频率附近，且随着转速的升高保持架质心涡动频率逐渐从大于保持架转动频率变为小于保持架转动频率。因此，为了避免保持架和引导套圈的接触发生在同一点或少数几点而导致保持架快速磨损，随着轴承工作转速的提升，必须关注保持架质心振动频率和保持架转动主频、分频及倍频的关系。

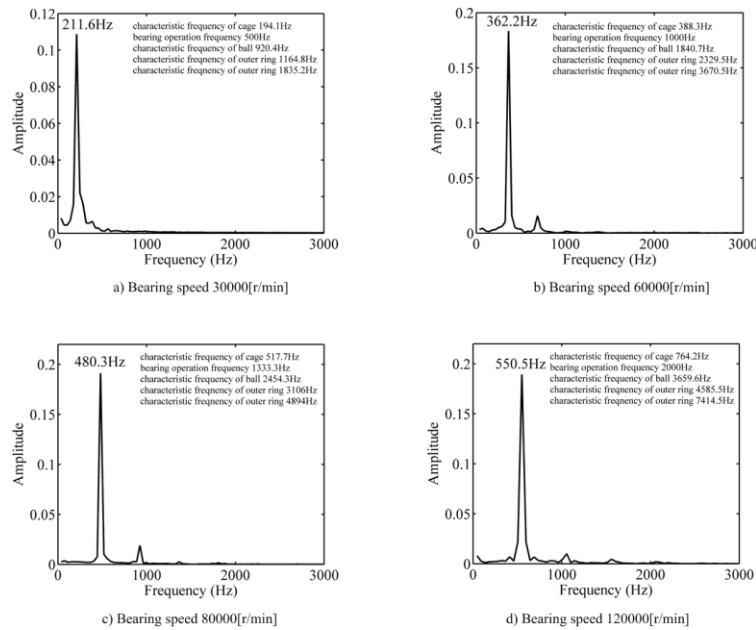


Fig. 11 - The spectrum of the cage center vibration at different bearing operation speed

Effect of changing bearing velocity on the dynamic performance of cage

According to the analysis results of the impact of different velocities on dynamic performance of the cage in the last section, it is clear that for different initial velocity, the changing processes of the bearing starting and the velocity increasing should be treated differently in terms of their impact on the dynamic performance of the cage.

Figure 12 shows the speeds of bearing elements during the starting process. It is indicated that the range of the speed of the rolling elements during the starting process follows the same trend of the speed ranges of the inner ring which shows a linear acceleration. However, there is stagnation and fluctuation of the cage speed within 6 ms while the bearing is started. This phenomenon can be ascribed by the fact that the cage speed relies entirely on the promotion of the rolling elements during the short period in which the bearing is started, and the relatively long interaction cycle between the cage and the rolling elements under the low velocity determines some delay of the cage starting. Meanwhile, the difference of speed between the rolling elements and the cage on the sudden start-up condition causes reciprocating collision between the cage pocket and the rolling element, leading to momentary velocity fluctuations of the cage during start-up.

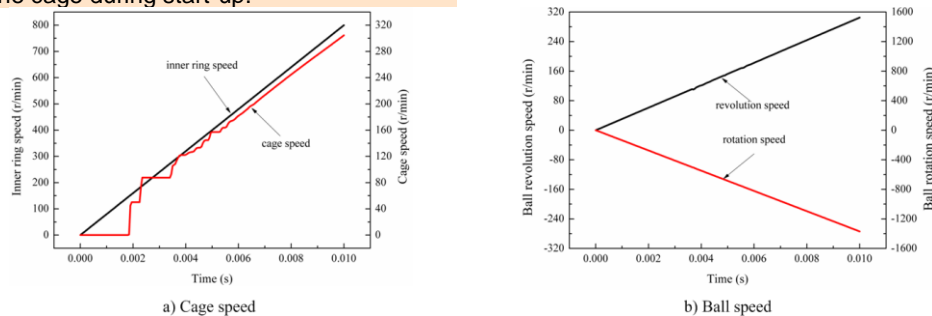


Fig. 12- Speed of the bearing elements during the beginning of their movement

Figure 13 shows the time response of the cage during the bearing starting process. According to Figure 13a, the impact of the cage pocket and the rolling element appears mainly in the short period when the cage is

转速变化过程对保持架动态性能影响

根据上一节不同转速对保持架动态性能影响的分析结果可知，轴承启动和轴承提速两个变化过程对保持架动态性能的影响由于初始转速不同需要区别对待。

图 12 所示为轴承启动过程中各元件的转速变化情况。从图中可见，轴承启动加速过程中滚动体的转速变化与轴承内圈速度变化趋势一致，呈现线性加速状态。但是保持架转速在轴承启动的 6ms 内存在停滞和波动现象，这是因为在轴承启动的短时期内保持架的运动加速完全依靠滚动体的推动作用，而低转速下滚动体和兜孔之间较长的相互作用周期决定了保持架的启动会出现一定的延迟，同时，突然启动的保持架与滚动体之间的速度差使得保持架兜孔和滚动体之间出现往复碰撞，使得刚启动的保持架出现短时的速度波动。

图 13 所示为轴承启动过程中保持架的受力情况。据图 13a)可知，保持架兜孔和滚动体的冲击主要出现在保持

starting-up, and the driving force of the rolling element to the cage weakens gradually with time, with the cage eventually reaching a stable stage. Meanwhile, it can be seen from Figure 13b that the impact of the guiding surface of the ring on the cage increases gradually, indicating that under the force of the rolling element, the cage is getting close to the guiding surface of the ring to achieve a new balance.

架启动的很短时间内，滚动体对保持架的推动力随着时间逐渐减弱，最终使得保持架启动进入平稳阶段。同时，从图 13b)可以看出，套圈引导面对保持架的作用逐渐增强，说明保持架在滚动体的作用下会向套圈引导面靠近从而寻找新的平衡。

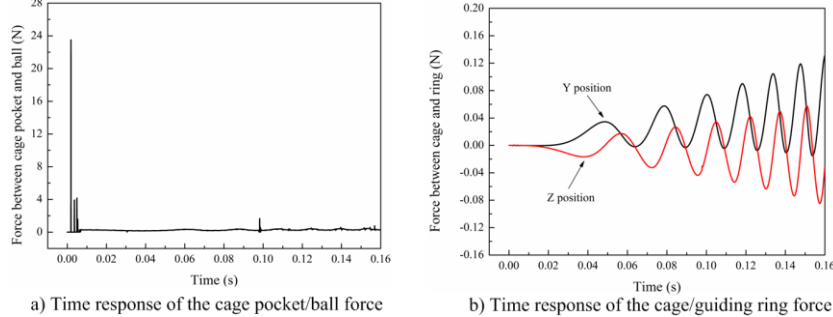


Fig. 13 - Load vibration of cage in the bearing starting process

Fig. 14 shows the speed of bearing elements when the speed of inner ring ranges from 80000 - 85000 rot/min. As the figure shows, when the velocity of the bearing is accelerated under high-speed operation, the velocity of the rolling elements and the cage shows a fluctuating rising state, which is different from that of the bearing starting process. The main reasons that are the frequent collision of the rolling element and the cage pocket under a high velocity as well as the centrifugal force generated at a high velocity have an influence on the internal load distribution of the bearings which causes a difference among the traction force of the rolling elements at different azimuths.

图 14 所示为轴承内圈从 80000r/min 加速到 85000r/min 的过程中各元件的转速变化情况。从图中可以看出，轴承在高速运转情况下进一步加速时滚动体和保持架的转速都呈现波动上升的状态，与轴承启动加速过程中的情况不同。这是因为滚动体和套圈兜孔在高速情况下发生碰撞接触的频率增大，同时高速产生的离心力对轴承内部载荷分布的影响导致滚动体在不同方位下受到的套圈拖动力存在差异，二者的共同作用最终导致滚动体在加速过程中出现不规则的速度波动。

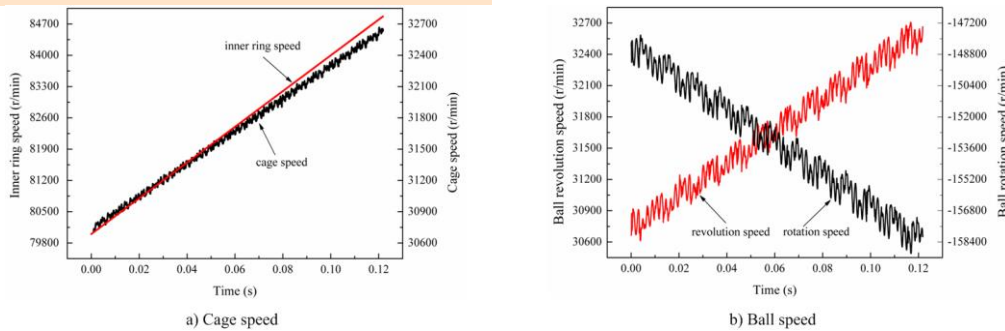


Fig. 14 - Speed of bearing element in bearing acceleration process

Fig. 15 shows the spectra of the interaction between the cage and the rolling element as well as the interaction between the cage and the guiding ring during the bearing acceleration process.

图 15 给出了提速过程中保持架和滚动体以及套圈间相互作用的频谱。

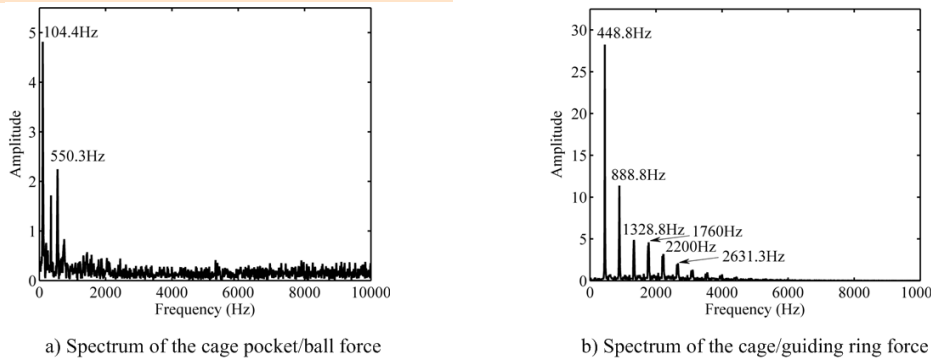


Fig. 15 - Load spectra of cage in bearing acceleration process

As shown in Fig. 15, despite the spectral peaks appearing in the force spectrum of the interaction between the cage and the rolling element, broadband noise still exists. Therefore, there is a random impact process in the interaction between the cage and the rolling element in the bearing acceleration conditions with high speed. Meanwhile, multi-cycle vibration characteristics occur in the interaction between the cage and the guiding ring, indicating that the guiding effect of the ring to the cage is obvious when the bearing is accelerated.

CONCLUSIONS

In this paper, a dynamics analysis model of high-speed ball bearings is established, the reliability of which is verified by using the experimental examples of Gupta. The model can be used for the steady and transitional dynamic analysis for bearings under different working conditions, which provides a theoretical tool for the design of working conditions and failure analysis of high-speed ball bearings in the transmission systems of agricultural machinery. Though analysis of the effects of velocity changes on the stability of the dynamic performance of high-speed ball bearings, there are some conclusions that have been reached:

(1) As the velocity increases, the vibrational frequency of the cage mass center changes from being higher than the cage rotation frequency to be lower than it. Thus, in order to avoid the contact between the cage and the guiding ring being restricted in only one place or several places which would cause rapid wear of the cage, the relationship between the cage whirl frequency and the main frequency, the sub-frequency, the multi-frequency of the cage must be analyzed during actual operation.

(2) The cage suffers from periodic impact of the rolling elements during the startup phase of the bearing, which causes the cage to be in an unstable state. However, when the bearing is moving high-speed, bearing acceleration has no significant effect on the stability of the cage.

ACKNOWLEDGEMENT

The work has received support from the National Natural Science Foundation of China (51375108), Science and Technology Foundation of GuiZhou Province of China (Qian Ke He J Zi [2014]2172) and Natural Science Research Project of Education Department of GuiZhou Province of China (Qian Jiao He KY Zi [2014]294).

REFERENCES

- [1]. Baomin Wang, Xuesong Mei, Chibing Hu, Zaixin Wu., (2008) – *Contact Angular Calculation and Analysis of High-Speed Angular Contact Ball Bearing*, Transactions of the Chinese Society for Agricultural Machinery, vol.39, no.9, pp.174-178;
- [2]. Bing Fang, Lei Zhang, Xingtian Qu, Ji Zhao., (2012) – *Dynamic Modeling and Experiment of Angular Contact Ball Bearing*, Transactions of the Chinese Society for Agricultural Machinery, vol.43, no.6, pp.215-219;
- [3]. Changqing Bai, Qingyu Xu., (2006) - *Dynamic Model of Ball Bearings with Internal Clearance and Waviness*, Journal of Sound and Vibration, vol.294, pp.23-28;
- [4]. Chendong Duan, Yan Guo., (2008) – *An Envelop Analysis Approach for Ball Bearing Based on Lifting Wavelet Packet Transform*, Transactions of the Chinese Society for

从图 15 可以看出, 保持架兜孔和滚动体之间的作用力频谱虽然出现了频谱峰值但是周围存在宽频噪声, 所以高速提速情况下保持架和兜孔之间的作用依然存在随机的冲击过程。保持架和套圈引导面之间的作用呈现多周期振动的特点, 说明在提速情况下套圈引导面对保持架的引导作用明显。

结论

本文建立了高速球轴承的动力学分析模型并采用 Gupta 实验算例验证了本文模型的可靠性, 模型可针对不同工况条件下轴承的稳态及瞬态过渡进行动力学分析, 为农机传动系统中高速球轴承的设计以及失效分析提供了理论工具。通过分析转速变化对高速球轴承动态性能稳定性影响, 得出以下结论:

(1) 随着转速的升高, 保持架质心振动频率逐渐从大于保持架转动频率变为小于保持架转动频率, 为避免保持架和引导套圈的接触发生在同一点或少数几点而导致保持架快速磨损, 在实际工作中必须对保持架质心振动频率与保持架转动主频、分频及倍频的关系进行分析。

(2) 轴承在加速启动阶段保持架受到滚动体周期性的冲击, 使保持架处于不稳定状态, 而当轴承处于高速阶段时转速的提升对保持架的稳定性没有明显的影响。

致谢

本文的研究获得了国家自然科学基金项目 (51375108), 贵州省科学技术基金 (黔科合 J 字 [2014]2172), 贵州省教育厅自然科学研究项目 (黔教合 KY 字 [2014]294) 的资助。

参考文献

- [1]. 王保民, 梅雪松, 胡赤兵, 鄢再新. (2008) – *高速角接触球轴承接触角计算与影响因素分析*, 农业机械学报, 第 39 卷, 第 9 期, 174-178;
- [2]. 方兵, 张雷, 曲兴田, 赵继. (2012) – *角接触球轴承动力学建模与实验*, 农业机械学报, 第 43 卷, 第 6 期, 215-219;
- [3]. 白长青, 许庆余. (2006) - *带有内部游隙和表面波纹度的球轴承动力学模型*, 声音与振动, 第 294 卷, 23-28;
- [4]. 段晨东, 郭研. (2008) – *基于提升小波包变换的滚动轴承包络分析诊断方法*, 农业机械学报, 第 39 卷, 第 5 期, 192-196;

Agricultural Machinery, vol.39, no.5, pp.192-196;

[5]. Chunjiang Zhao, Guohua Cui, Guoqiang Wang, Qingxue Huang, Fangping Zhang., (2008) – *Precise Definition of Contact Angle Field on High Speed Angular-Contact Ball Bearing under Axial Load*, Transactions of the Chinese Society for Agricultural Machinery, vol.39, no.12, pp.153-156;

[6]. Ghaisas N., Wassgren C. R., Sadeghi F., (2004) - *Cage Instabilities in Cylindrical Roller Bearings*, Journal of tribology, vol.126, pp.681-689;

[7]. Gupta, P. K., (1991) - *Modeling of Instabilities Induced by Cage Clearances in Ball Bearings*, Tribology Transactions, vol.34, no.1, pp.93-99;

[8]. Gupta P. K., (1984) - *Advanced Dynamic of Rolling Elements*, Springer-Verlag, New York;

[9]. Hamrock B. J., Dowson D., (1981) - *Ball Bearing Lubrication: The Elastohydrodynamics of Elliptical Contacts*, John Wiley, New York;

[10]. Johnson K. L., (1992) - *Contact Mechanics*, Cambridge University Press, Cambridge;

[11]. Jun Zhang, Senlin LU, Weixing He, Yishun Wang, Tianbo Li., (2007) – *Vibration Diagnosis of Rolling Bearings Based on Wavelet Packet Energy Feature*, Transactions of the Chinese Society for Agricultural Machinery, vol.38, no.10, pp.178-181;

[12]. Liqin Wang, Li Cui, Dezhi Zheng, Le Gu., (2007) - *Analysis on Dynamic Characteristics of Aero-Engine High-Speed Ball Bearings*, Acta Aeronautica et Astronautica Sinica, vol.28, no.6, pp.1461-1467;

[13]. Mingming Li, (2013) – *Upgrade Path of China Agricultural Industry (Continued 1)*, Farm Machinery, no.22, pp. 48-56;

[14]. Preda I., Ciolan Gh., (2013) – *Algorithm to Define the Speed Ratios of the Tractor Complex Geartrains*, INMATEH–Agricultural Engineering, vol.41, no.3, pp.77-84;

[15]. Schlichting, H., Translated by Kestin, J. (1979) - *Boundary-Layer Theory*, McGraw-Hill Inc., New York;

[16]. Villa D., Gazzola J., Dal Fabbro I. M., Silva M. V.G. (2014) – *Moir Supported Stress Distribution Study on Gears*, INMATEH – Agricultural Engineering, vol.44, no.3, pp.157-164;

[17]. Weinzapfel, N., Sadeghi, F., (2009) - *A Discrete Element Approach for Modeling Cage Flexibility in Ball Bearing Dynamics Simulations*, Journal of Tribology, vol.131, no.2: 021102;

[18]. Xianqi Yang, Wenxiu Liu, Xiaoling Li, (2002) – *Dynamic Analysis on Cage of High Speed Roller Bearing*, Bearing, no.7, pp.1-5;

[19]. Xiuhai Liu, Sier Deng, Hongfei Teng, (2011) - *Dynamic Stability Analysis of Cages in High-Speed Oil-Lubricated Angular Contact Ball Bearings*, Transactions of Tianjin University, vol.17, no.1, pp.20-27;

[20]. Yanshuang Wang, Boyuan Yang, Liqin Wang, Peibin Zheng, (2004) - *Traction Behavior of 4106 Aviation Lubricating Oil*, Tribology, vol.24, no.2, pp.156-159;

[21]. Yaobin Zhuo, Xiaojun Zhou, (2013) – *Analysis of Effect of Clearance on Static Mechanical Behavior for Double Row Self-Aligning Ball Bearing and Control of Clearance*, Transactions of the Chinese Society of Agricultural Engineering, vol.29, no.19, pp.63-70;

[22]. Yonggang Xu, Zhipeng Meng, Ming Lu, (2013) – *Fault Diagnosis of Rolling Bearing Based on Dual-Tree Complex Wavelet Packet Transform*, Transactions of the Chinese Society of Agricultural Engineering, vol.29, no.10, pp.49-56;

[5]. 赵春江, 崔国华, 王国强, 黄庆学, 张芳萍. (2008) – *轴向受载的高速角接触球轴承接触角域的精确确定*, 农业机械学报, 第 39 卷, 第 12 期, 153-156;

[6]. Ghaisas, N., Wassgren, C. R., Sadeghi, F. (2004) – *援助滚子轴承的保持架不稳定性分析*, 美国摩擦学报, 第 126 卷, 681-689;

[7]. Gupta, P. K. (1991) - *保持架间隙导致球轴承不稳定的分析模型*, 美国摩擦学会会刊, 第 34 卷, 第 1 期, 93-99;

[8]. Gupta, P. K. (1984) – *滚动轴承高等动力学*, 施普林格出版社, 纽约;

[9]. Hamrock, B. J., Dowson, D. (1981) – *球轴承的润滑: 椭圆接触的流体动压润滑*, 约翰威立出版社, 纽约;

[10]. Johnson, K. L. (1992) – *接触力学*, 剑桥大学出版社, 剑桥;

[11]. 张军, 陆森林, 和卫星, 王以顺, 李天博. (2007) – *基于小波包能量法的滚动轴承故障诊断*, 农业机械学报, 第 38 卷, 第 10 期, 178-181;

[12]. 王黎钦, 崔立, 郑德志, 古乐. (2007) - *航空发动机高速球轴承动态特性分析*, 航空学报, 第 28 卷, 第 6 期, 1461-1467;

[13]. 李明明. (2013) – *中国农机工业的升级路 (续1)*, 农业机械, 第 22 期, 48-56;

[14]. Preda I., Ciolan Gh. (2013) – *拖拉机复杂齿轮系速度比定义的算法*, INMATEH – 农业工程, 第 41 卷, 第 3 期, 77-84.

[15]. Schlichting, H. 著, Kestin, J. 翻译 (1979) – *边界层理论*, 麦格劳-希尔出版社, 纽约;

[16]. Villa D., Gazzola J., Dal Fabbro I. M., Silva M. V.G. (2014) – *齿轮莫尔支承应力分布研究*, INMATEH – 农业工程, 第 44 卷, 第 3 期, 157-164.

[17]. Weinzapfel, N., Sadeghi, F. (2009) – *球轴承柔性保持架动力学仿真的离散单元法*, 美国摩擦学报, 第 131 卷, 第 2 期, 021102;

[18]. 杨咸启, 刘文秀, 李晓玲. (2002) - *高速滚子轴承保持架动力学分析*, 轴承, 第 7 期, 1-5;

[19]. 刘秀海, 邓四二, 腾弘飞. (2011) – *高速油润滑角接触球轴承的保持架动态稳定性分析*, 天津大学学报, 第 17 卷, 第 1 期, 20-27;

[20]. 王燕霜, 杨伯原, 王黎钦, 郑培斌. (2004) – *4106 航空润滑油拖动特性研究*, 摩擦学报, 第 24 卷, 第 2 期, 156-159;

[21]. 卓耀彬, 周晓军. (2013) – *游隙对双列调心球轴承静力学性能影响及游隙控制分析*, 农业工程学报, 第 29 卷, 第 19 期, 63-70;

[22]. 胥永刚, 孟志鹏, 陆明. (2013) – *基于双树复小波包变换的滚动轴承故障诊断*, 农业工程学报, 第 29 卷, 第 10 期, 49-56.